Pressure induced electronic phase transitions and superconductivity in n-type Bi$_2$Te$_3$

Junliang Zhang, Sijia Zhang, Panpan Kong, Liuxiang Yang, Changqing Jin, Qingqing Liu, Xiancheng Wang, and Jiancheng Yu

---

Articles you may be interested in

Pressure induced electronic phase transitions and superconductivity in n-type Bi$_2$Te$_3$

Junliang Zhang,[1,a)] Sijia Zhang,[2] Panpan Kong,[2,3] Liuxiang Yang,[2,4,5] Changqing Jin,[2,6,b)] Qingqing Liu,[2] Xiancheng Wang,[2] and Jiancheng Yu[1]

[1]*Faculty of Electrical Engineering and Computer Science, Ningbo University, Ningbo 315211, People's Republic of China*
[2]*Institute of Physics, Chinese Academy of Sciences, Beijing 100190, China*
[3]*Max-Planck-Institut für Chemie, 55128 Mainz, Germany*
[4]*Carnegie Institution for Science, Geophysical Laboratory, High Pressure Synergetic Consortium, Argonne, Illinois 60439, USA*
[5]*Center for High Pressure Science and Technology and Advanced Research, Beijing 100094, China*
[6]*School of Physical Sciences, University of Chinese Academy of Sciences, Beijing 100190, China*

Temperature dependent-electrical resistance of n-type Bi$_2$Te$_3$ was investigated under high pressure. Superconductivity was detected at 4.9 GPa with $T_c^{onset} = 2.8$ K. Resistance and T_c suggest that there are two electronic phase transitions below 10 GPa. We conjecture that the bulk insulating phase first changes to semimetal and then to metal. The evolution of the Hall coefficient is qualitatively consistent with the proposed electronic phase transition. The origin of superconductivity and topological properties are also discussed. *Published by AIP Publishing.*
https://doi.org/10.1063/1.4997967

I. INTRODUCTION

Majorana fermions, fermions that are their own antiparticles, obey non-Abelian statistics which allow them to have potential applications in quantum computing.[1–3] It is theoretically predicted that Majorana fermions can be found in topological superconductors.[4–6] Similar to topological insulators, topological superconductors are a class of topological materials which have bulk superconductivity states along with gapless surface states protected by time-reverse symmetry.[7–10] These novel states can be found at the interfaces between topological insulators and s-wave superconductors due to the superconducting proximity effect.[11–14] Superconductivity can be realized in many topological compounds by chemical doping[15–17] or applying pressure.[13,18] Superconducting bulk states together with Dirac-type surface states could approach topological superconductors.

Bi$_2$Te$_3$, Bi$_2$Se$_3$, and Sb$_2$Te$_3$ are three typical 3D topological insulators which were theoretically[19] and experimentally demonstrated.[20–22] They have a similar rhombohedral structure with the space group of R-3m (No. 166) at atmospheric pressure. Superconductivity was detected in the rhombohedral phase of p-type Bi$_2$Te$_3$ and p-type Sb$_2$Te$_3$ under high pressure.[13,18,23,24] These materials are probably topological superconductors due to the three-fold symmetry of hole pockets. However, no superconductivity was found in undoped n-type Bi$_2$Se$_3$ before the structural phase transition.[25,26] Einaga reported the superconductivity transition in the R-3m structure of polycrystalline n-type Bi$_{35}$Te$_{65}$; however, their specimen is a Bi-Te alloy in which Bi and Te atoms are distributed homogeneously.[27]

In this study, we report resistance and Hall coefficients of n-type Bi$_2$Te$_3$ up to 10 GPa. Superconductivity is observed above 4.9 GPa. The variations of resistance and carrier concentration suggest that two electronic phase transitions take place at 4.9 GPa and 7 GPa, respectively. We discussed the pressure induced band structure evolution and electronic phase transition.

II. EXPERIMENTS

Bi$_2$Te$_3$ crystals were prepared by the Bridgeman method.[23,28] According to the Bi-Te phase diagram, the synthesis of n samples requires an excess of Te.[28] High-purity Bi (99.999%) and Te (99.999%) powders with a Bi/Te molar ratio of 0.6:1 were mixed, ground, and pressed into pellets. The pellets were then loaded into a quartz Bridgeman ampoule. The ampoule was evacuated, sealed, placed into a furnace, and heated at 800 °C for 3 days, after which it was slowly cooled in a temperature gradient at the rate 5 °C per hour to 300 °C, followed by furnace cooling. The final crystal is a silver bulk with a gray thin layer on the upper surface. Specimens were torn off from the silver part of the as grown crystal. The Bi/Te atomic ratio of 0.67:1 was analyzed by inductively coupled plasma emission spectroscopy (ICP). Powder X-ray diffraction (XRD) data were obtained by a Phillips X'PERT using Cu K$_{\alpha1}$ radiation ($\lambda = 1.54056$ Å). Fine powder was ground from specimens. All peaks can be indexed with rhombohedral structure Bi$_2$Te$_3$ with lattice parameters of a = b = 4.3852 Å, c = 30.483 Å, $\alpha = \beta = 90°$, and $\gamma = 120°$ [as shown in Fig. 1(a)]. The structure is the same as that of the p-type ones. The Hall coefficient at atmospheric pressure was measured by the four point probe method at 2 K in the MagLab system. The thickness of the specimen is 10 μm. Magnetic field H was perpendicular to

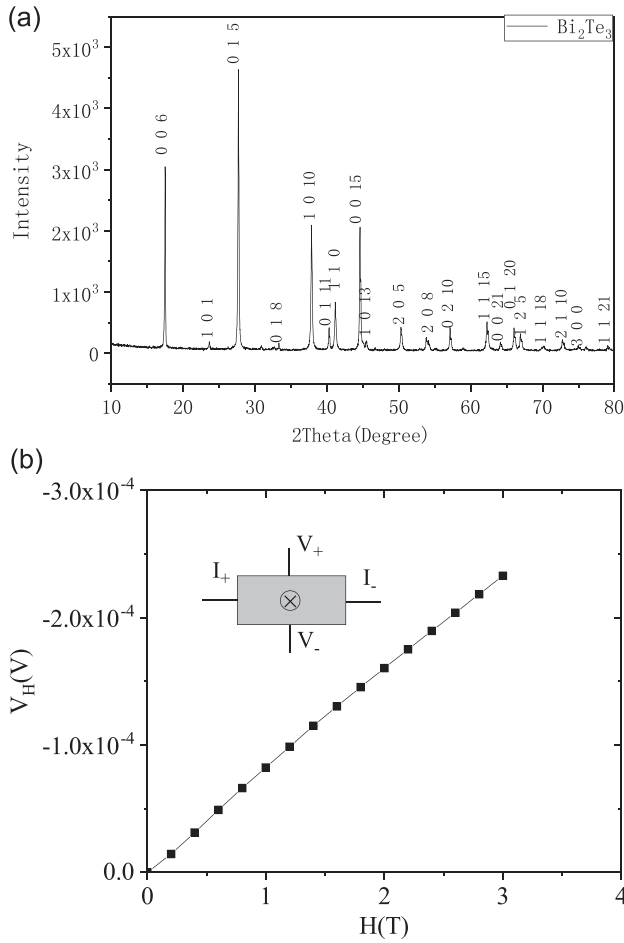a)Author to whom correspondence should be addressed: zhangjunliang@nbu.edu.cn
b)jin@iphy.ac.cn

(a)

(b)

FIG. 1. (a) Powder X-ray diffraction of Bi_2Te_3. (b) The Hall voltage of the Bi_2Te_3 at 2 K under atmospheric pressure with magnetic field H perpendicular to the ab-plane of the single crystal. The inset is a schematic of Hall coefficient measurement.

the ab-plane of the single crystal. The N-type carrier was deduced from the sign of the Hall coefficient and the concentration is around 7×10^{19}/cm^3 calculated from the Hall coefficient [Fig. 1(b)].

Resistances under high pressure were performed by four-probe methods in a diamond anvil cell (DAC) made of the CuBe alloy. Pressure was generated by a pair of diamonds with a 500 μm diameter culet. A gasket made of T301 stainless steel was pre-indented from the thickness of 250 μm to 60 μm, and a hole of 200 μm in diameter was drilled in the center of the pre-indented area. Cubic BN (c-BN) powder was pressed into the drilled hole and the pre-indented area as the insulating layer between the gasket and the electrodes. Another hole of about 130 μm in diameter was drilled in the center of the 200 μm hole. H-BN fine powder was then filled in this hole as pressure transmitting medium. A specimen with dimensions of 90 μm $\times$ 90 μm $\times$ 10 μm was put in the center of the hole. Slim Au electrodes with 18 μm in diameter were placed on the same side of the crystal. Two rubies were placed next to the specimen. Pressure was measured by ruby fluorescence method[29] at room temperature before each cooling. We investigated the pressure gradient within the sample chamber. The results show that the gradient is less than 10% within 50 μm from the center. The DAC was put inside a Mag

Lab system to perform the resistance and Hall coefficient measurements. The Hall coefficient was measured by using the Van der Pauw method. External magnetic field was applied by the Mag Lab system. Measurements of the high pressure Hall coefficient were performed at 2 K. As superconductivity has occurred above 4.9 GPa, the Hall coefficient was measured under high external field in order to destroy the superconducting states.

III. RESULTS AND DISCUSSION

Figures 2(a)–2(c) show temperature-dependent resistance under various pressures up to 10 GPa. The specimen shows metallic resistance behavior from 0 GPa to 2.0 GPa. For higher pressure up to 4.2 GPa, resistance shows metallic behavior at higher temperatures but changes to semiconductor-like behavior at lower temperatures. Resistance increases as pressure increases when the pressure is below 4.6 GPa. No superconductivity is detected below 4.6 GPa. Resistance at 4.9 GPa shows a fast drop with decreasing temperature at 182 K. Metallic temperature-dependent resistance was observed above 4.9 GPa up to 10 GPa. Resistance decreases rapidly with increasing pressure over the pressure range from 4.9 GPa to 7 GPa. Resistance increases with increasing pressure above 7 GPa.

Superconductivity initially appears at 4.9 GPa [see Figs. 2(d) and 2(e)] with critical temperature $T_c^{onset} = 2.8$ K. A broad peak appears just above the superconducting transition. Superconducting T_c derived from temperature-dependent resistance curves is shown in Fig. 2(f). T_c^{onset} and T_c^{mid} were defined as the temperatures at which resistances drop to 90% and 50% of the value before transition. T_c^{zero} was defined as the temperature at which resistance $\sim$0. Superconducting T_c is almost constant below 7 GPa, whereas T_c increases obviously with increasing pressure above 7 GPa. According to high pressure angle-dispersive powder X-ray diffraction (ADXRD) results at 8 K,[30] the ambient phase is stable up to 10 GPa. Therefore, the superconducting phase above 7 GPa is still the R-3m structure.

Resistance versus temperature as a function of magnetic field was measured to confirm whether the transitions are indeed superconducting transitions. Figure 3 shows the results under 5.3 GPa and 9.2 GPa. T_c shifts to the lower temperature side with increasing magnetic fields in both cases, which indicates that the transitions are superconductivity in nature. The resistance peak before transition also left shifts under magnetic fields, whereas that beyond the peak remains almost unchanged under fields. We believe that the peak has a certain connection with superconductivity. Figure 3(c) shows field-dependence of T_c^{mid}. The upper critical field $H_{c2}(0) = 0.42$ T under 5.3 GPa and $H_{c2}(0) = 6.46$ T under 9.2 GPa are both extrapolated by using the Wertheimer-Helfand-Hohenberg formula

$$H_{c2}(0) = -0.691 \left[\frac{dH_{c2}(T)}{dT} \right]_{T=T_c} \cdot T_c.$$

The upper critical field of superconducting phase under 5.3 GPa is much lower than that under 9.2 GPa. The difference
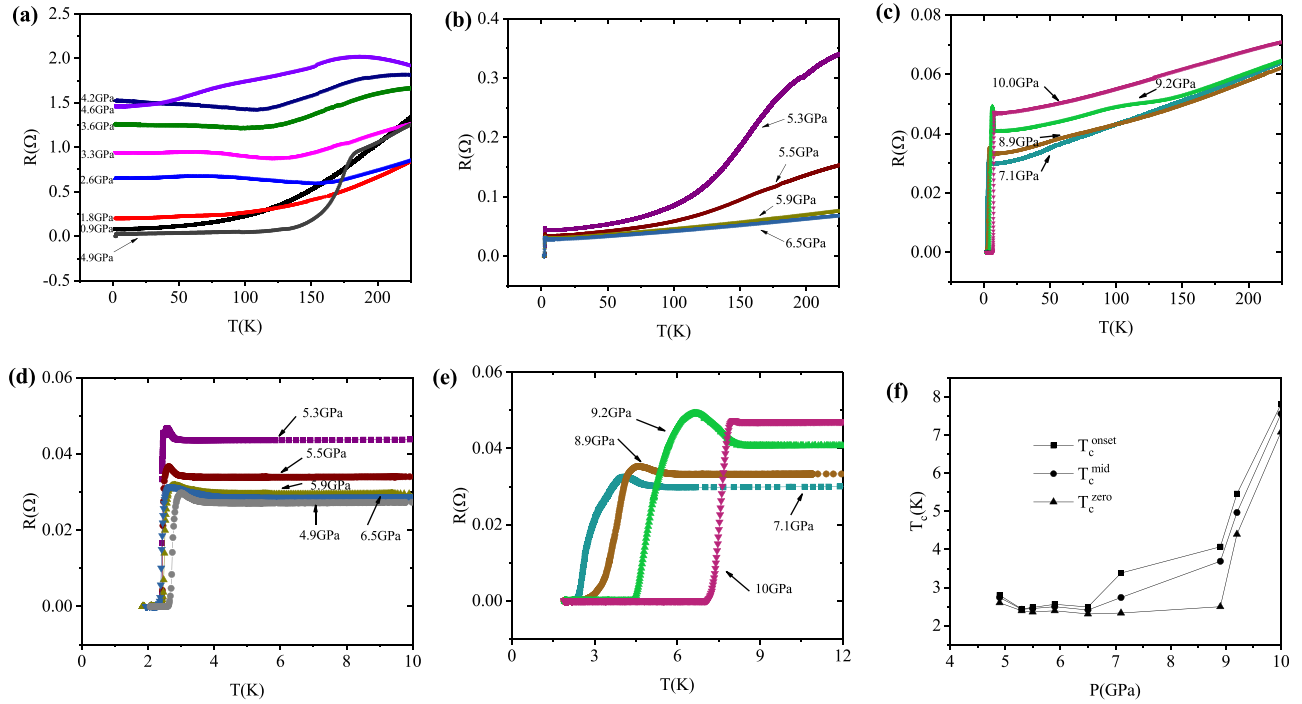
FIG. 2. (a), (b), and (c) Temperature-dependent resistance under high pressure. (d) and (e) are partial enlarged details on superconducting parts, respectively. (f) Pressure dependence of superconducting T_c.
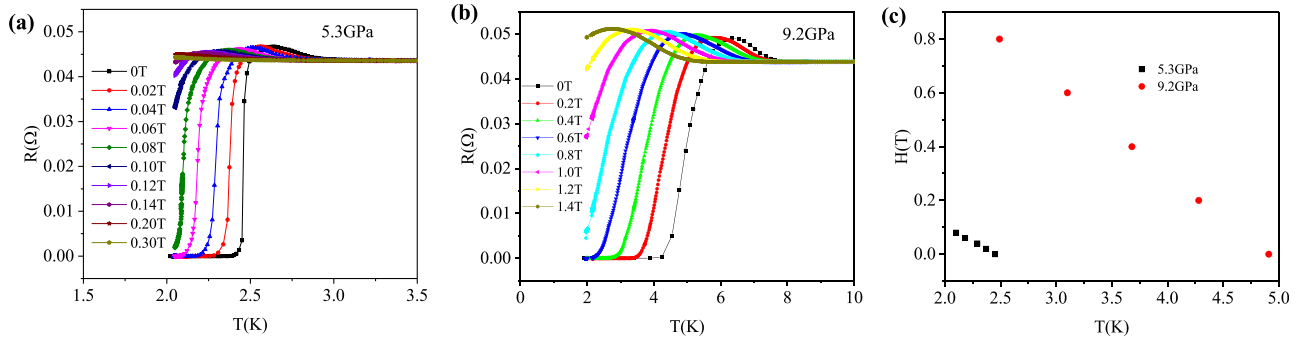

FIG. 3. Resistance versus temperature measured at different magnetic fields under (a) 5.3 GPa and (b) 9.2 GPa. (c) Middle point T_c at different fields.

in magnitude of upper critical field leads us to assume that the superconductivity mechanism at two pressures might be different.

The Hall coefficient was measured to check the carrier characteristics. The specimen remains n-type over the pressure range up to 10 GPa. Carrier concentration vs. pressure is shown in Fig. 4. Carrier concentration slowly decreases with increasing pressure below 4.3 GPa while increasing dramatically above 4.3 GPa. This means that there is an electronic phase transition around 4.3 GPa. In contrast to the resistance results, the transition pressure is about 4.6 GPa actually. The decrease of carrier concentration with increasing pressure is
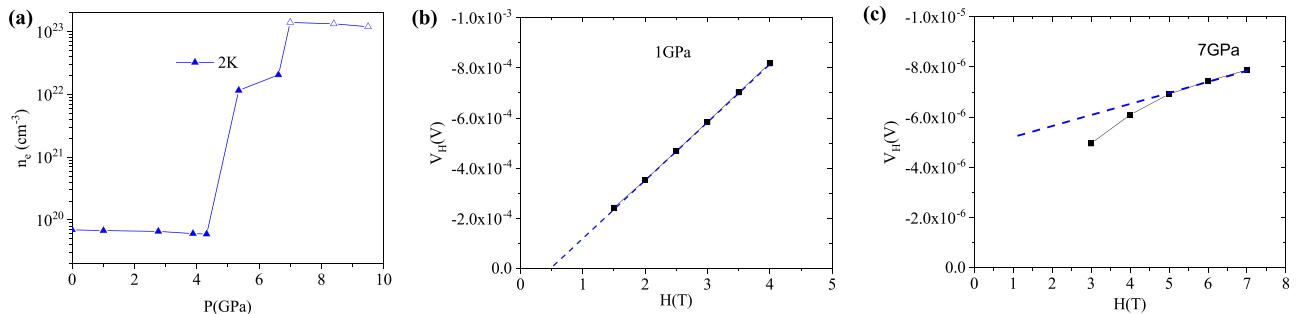

FIG. 4. (a) Pressure-dependent carrier concentration. ▲ indicates carrier concentration deduced from linear part V_H-H. △ indicates carrier concentration deduced from the slope of V_H-H above 7T. (b) and (c) The Hall voltage of the Bi_2Te_3 at 1 GPa and 7 GPa respectively. ■ indicates the experimental data. Blue dashed lines are the fitting of the linear parts.

probably due to the Fermi surface shift. Above 7 GPa, carrier concentration reaches a very high level. Hall voltage no longer varies linearly with magnetic field. Based on the slope of V_H-H near 7T, carrier concentration is deduced at the order of $10^{23}/cm^3$ magnitude. High carrier concentration demonstrated that the normal phase above T_c is a metallic phase.

Now we turn back to the normal phase above T_c between 4.6 GPa and 7 GPa. According to the band structures reported previously,[13,31] the conduction band minimum (CBM) and valence band maximum (VBM) of bulk states are located at different positions away from the Γ point. The CBM moves down and the VBM moves up under high pressure. Therefore, the band structure may transform to a semimetallic phase before they completely overlap in the compressing process. The evolution of the Hall coefficient is qualitatively consistent with the proposed electronic phase transition. Figure 5(a) shows the possible schematic diagram of band structure evolution. Figure 5(b) is the proposed pressure electronic phase diagram. However, the existence of the semimetal phase should be further confirmed by band structure calculations or experimental evidence.
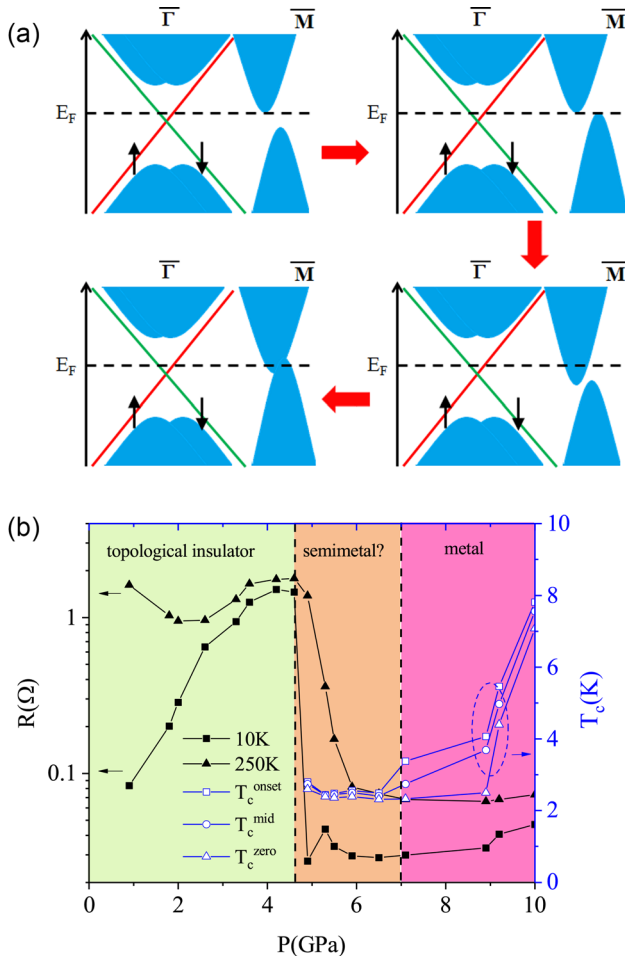
Superconductivity in n-type Bi_2Te_3 indicates that the carrier type does not play a major role in the superconductivity in Bi_2Se_3 class compounds. In the so-called semimetal phase of Bi_2Te_3, six bulk electron Fermi pockets coexist with six hole Fermi pockets. Due to the three-fold symmetry of the Fermi surface, the electron pockets or the hole pockets are three-fold symmetry. The pairing symmetry is triplet pairing symmetry similar to p-type Bi_2Te_3 or p-type Sb_2Te_3. In contrast to other compounds of Bi_2Se_3 class, only Bi_2Se_3 is a direct gap semiconductor. It has just one electron (hole) pocket at the Γ point. This may be the reason why Bi_2Se_3 has no superconducting phase in the R-3m structure.

Finally, we discuss the topological properties of the superconducting phases. The Dirac cones are located at the Γ point. The direct gap at the Γ point enhances under pressure. This means that the Dirac cone remains even though the conduction band meets the valence band at other points. Topological superconductivity can be realized on surface states due to the superconducting proximity effect. For the superconducting phase above 7 GPa, the bulk states transform from the semiconductor to metal. However, the Dirac cone of surface states probably remains well defined at the Γ point. If so, it is also a candidate of topological superconductor.

IV. CONCLUSIONS

In conclusion, we have investigated temperature-dependent electrical resistance of n-type Bi_2Te_3 under high pressure. The superconductivity was detected at 4.9 GPa with $T_c^{onset} = 2.8$ K. The n-type carriers were suggested by the sign of the Hall coefficient. Two electronic phase transitions are observed below 10 GPa. We conjecture that the bulk insulating phase first changes to semimetal and then to metal. The evolution of the Hall coefficient is qualitatively consistent with the proposed electronic phase transition. The superconducting origin and topological properties are also discussed.

FIG. 5. (a) Schematic energy diagram of possible bulk states revolution of n-type Bi_2Te_3. Blue lumps indicate the bulk states, and red lines and green lines indicate the surface states of spin up and spin down, respectively. (b) Pressure dependence of resistance (left Y-axis) and superconducting T_c (right Y-axis), different electronic phase are distinguished with different background colors.

[1]T. Hyart, B. van Heck, I. C. Fulga, M. Burrello, A. R. Akhmerov, and C. W. J. Beenakker, Phys. Rev. B **88**, 035121 (2013).
[2]K. Flensberg, Phys. Rev. Lett. **106**, 090503 (2011).
[3]A. R. Akhmerov, Phys. Rev. B **82**, 020509 (2010).
[4]X.-L. Qi and S.-C. Zhang, Rev. Mod. Phys. **83**, 1057–1110 (2011).
[5]M. Leijnse and K. Flensberg, Semicond. Sci. Technol. **27**, 124003 (2012).
[6]S. R. Elliott and M. Franz, Rev. Mod. Phys. **87**, 137–163 (2015).
[7]M. Sato and Y. Ando, Rep. Prog. Phys. **80**, 076501 (2017).
[8]D. Meidan, E. Berg, and A. Stern, Phys. Rev. B **95**, 205104 (2017).
[9]A. P. Schnyder, S. Ryu, A. Furusaki, and A. W. W. Ludwig, Phys. Rev. B **78**, 195125 (2008).
[10]X.-L. Qi, T. L. Hughes, S. Raghu, and S.-C. Zhang, Phys. Rev. Lett. **102**, 187001 (2009).
[11]L. Fu and C. L. Kane, Phys. Rev. Lett. **100**, 096407 (2008).
[12]T. D. Stanescu, J. D. Sau, R. M. Lutchyn, and S. Das Sarma, Phys. Rev. B **81**, 241310 (2010).

[13]J. L. Zhang, S. J. Zhang, H. M. Weng, W. Zhang, L. X. Yang, Q. Q. Liu, S. M. Feng, X. C. Wang, R. C. Yu, L. Z. Cao, L. Wang, W. G. Yang, H. Z. Liu, W. Y. Zhao, S. C. Zhang, X. Dai, Z. Fang, and C. Q. Jin, Proc. Natl. Acad. Sci. U.S.A. **108**, 24–28 (2011).

[14]J. D. Sau, R. M. Lutchyn, S. Tewari, and S. Das Sarma, Phys. Rev. B **82**, 094522 (2010).

[15]Y. S. Hor, A. J. Williams, J. G. Checkelsky, P. Roushan, J. Seo, Q. Xu, H. W. Zandbergen, A. Yazdani, N. P. Ong, and R. J. Cava, Phys. Rev. Lett. **104**, 057001 (2010).

[16]Z. Wang, A. A. Taskin, T. Frolich, M. Braden, and Y. Ando, Chem. Mater. **28**, 779–784 (2016).

[17]S. Sasaki and T. Mizushima, Physica C **514**, 206–217 (2015).

[18]J. Zhu, J. L. Zhang, P. P. Kong, S. J. Zhang, X. H. Yu, J. L. Zhu, Q. Q. Liu, X. Li, R. C. Yu, R. Ahuja, W. G. Yang, G. Y. Shen, H. K. Mao, H. M. Weng, X. Dai, Z. Fang, Y. S. Zhao, and C. Q. Jin, Sci. Rep. **3**, 2016 (2013).

[19]H. Zhang, C.-X. Liu, X.-L. Qi, X. Dai, Z. Fang, and S.-C. Zhang, Nat. Phys. **5**, 438–442 (2009).

[20]Y. L. Chen, J. G. Analytis, J. H. Chu, Z. K. Liu, S. K. Mo, X. L. Qi, H. J. Zhang, D. H. Lu, X. Dai, Z. Fang, S. C. Zhang, I. R. Fisher, Z. Hussain, and Z. X. Shen, Science **325**, 178–181 (2009).

[21]Y. Xia, D. Qian, D. Hsieh, L. Wray, A. Pal, H. Lin, A. Bansil, D. Grauer, Y. S. Hor, R. J. Cava, and M. Z. Hasan, Nat. Phys. **5**, 398–402 (2009).

[22]D. Hsieh, Y. Xia, D. Qian, L. Wray, F. Meier, J. H. Dil, J. Osterwalder, L. Patthey, A. V. Fedorov, H. Lin, A. Bansil, D. Grauer, Y. S. Hor, R. J. Cava, and M. Z. Hasan, Phys. Rev. Lett. **103**, 146401 (2009).

[23]S. J. Zhang, J. L. Zhang, X. H. Yu, J. Zhu, P. P. Kong, S. M. Feng, Q. Q. Liu, L. X. Yang, X. C. Wang, L. Z. Cao, W. G. Yang, L. Wang, H. K. Mao, Y. S. Zhao, H. Z. Liu, X. Dai, Z. Fang, S. C. Zhang, and C. Q. Jin, J. Appl. Phys. **111**, 112630 (2012).

[24]C. Zhang, L. Sun, Z. Chen, X. Zhou, Q. Wu, W. Yi, J. Guo, X. Dong, and Z. Zhao, Phys. Rev. B **83**, 140504 (2011).

[25]K. Kirshenbaum, P. S. Syers, A. P. Hope, N. P. Butch, J. R. Jeffries, S. T. Weir, J. J. Hamlin, M. B. Maple, Y. K. Vohra, and J. Paglione, Phys. Rev. Lett. **111**, 087001 (2013).

[26]P. P. Kong, J. L. Zhang, S. J. Zhang, J. Zhu, Q. Q. Liu, R. C. Yu, Z. Fang, C. Q. Jin, W. G. Yang, X. H. Yu, J. L. Zhu, and Y. S. Zhao, J. Phys.: Condens. Matter **25**, 362204 (2013).

[27]M. Einaga, A. Ohmura, F. Ishikawa, A. Nakayama, Y. Yamada, S. Nakano, A. Matsushita, and K. Shimizu, J. Phys.: Conf. Ser. **500**, 192003 (2014).

[28]C. B. Satterthwaite and R. W. Ure, Jr., Phys. Rev. **108**, 1164 (1957).

[29]H. K. Mao, J. Xu, and P. M. Bell, J. Geophys. Res.: Solid Earth **91**, 4673–4676, https://doi.org/10.1029/JB091iB05p04673 (1986).

[30]J. L. Zhang, S. J. Zhang, J. L. Zhu, Q. Q. Liu, X. C. Wang, C. Q. Jin, and J. C. Yu, Physica B **521**, 13–16 (2017).

[31]K. Zhao, Y. Wang, C. Xin, Y. Sui, X. J. Wang, Y. Wang, Z. G. Liu, and B. S. Li, J. Alloys Compd. **661**, 428–434 (2016).